Available online at www.sciencedirect.com
SCIENCE DIRECT®
Postharvest Biology and Technology 30 (2003) 29–42
Postharvest Biology and Technology
www.elsevier.com/locate/postharvbio

A respiration–diffusion model for 'Conference' pears I: model development and validation

J. Lammertyn [a,*], N. Scheerlinck [a], P. Jancsók [b], B.E. Verlinden [a], B.M. Nicolaï [a]

[a] *Department of Agro Engineering and -Economics, Flanders Centre/Laboratory of Postharvest Technology, Catholic University Leuven, Willem de Croylaan 42, B-3001 Leuven, Belgium*

[b] *Department of Agro Engineering and -Economics, Laboratory of Agro-Machinery and Processing, Catholic University Leuven, Kasteelpark Arenberg 30, B-3001 Leuven, Belgium*

Received 14 August 2002; accepted 23 March 2003

Abstract

A respiration–diffusion model based on Fick's second law of diffusion and Michaelis–Menten kinetics, including non-competitive CO_2 inhibition, was developed to predict the internal O_2 and CO_2 concentrations in 'Conference' pears. The 'respiration-free' diffusion and 'diffusion-free' respiration parameters, determined in previous independent experiments, were incorporated in the respiration–diffusion model. The system of coupled non-linear partial differential equations was solved numerically for a three-dimensional pear geometry, by means of the finite element method. When Michaelis–Menten kinetics are used to describe a process like gas exchange of fruits, which involves both gas diffusion and respiration, the Michaelis–Menten parameters were assigned a higher value than those obtained when respiration was first uncoupled from the diffusion process and then described by means of Michaelis–Menten kinetics. The maximal O_2 consumption and fermentative CO_2 production were diffusion-independent, but the Michaelis–Menten constants measured on cell protoplasts were considerably smaller when compared with the corresponding apparent Michaelis–Menten constants determined from respiration measurements on intact pears. The model was successfully validated for its prediction of the total pear gas exchange and the gas concentration under the skin, and is suited to simulating three-dimensional internal O_2 and CO_2 dioxide profiles in pears as a function of the storage atmosphere.

Keywords: Controlled atmosphere; Storage; *Pyrus communis* L.; Finite elements

1. Introduction

The term 'respiration' is often used to refer to the total gas exchange of the fruit with its environment. However, this gas exchange is in reality determined by the joint effect of respiration

* Corresponding author. Tel.: +32-16-32-2376; fax: +32-16-32-2955.
E-mail address: jeroen.lammertyn@agr.kuleuven.ac.be (J. Lammertyn).

0925-5214/03/$ - see front matter © 2003 Elsevier B.V. All rights reserved.
doi:10.1016/S0925-5214(03)00061-9

at the cellular level and gas diffusion through the pear tissue and skin (Cameron et al., 1995; Peppelenbos, 1996). Due to diffusion barriers between the ambient atmosphere and the cells, where respiration takes place, considerable gas gradients between the external and internal atmospheres may occur (Rajapakse et al., 1990). The O_2 and CO_2 concentration may, respectively, therefore, locally decrease beyond and, increase above some threshold values, which may trigger the cell degradation processes, which eventually will cause storage disorders such as core breakdown (Lammertyn, 2001). It is, therefore, important to know the local O_2 and CO_2 concentrations in the pear (*Pyrus communis* L. cv. Conference). A model-based approach is advantageous because the experimental determination of the local O_2 and CO_2 concentrations is not simple. Further, when a validated model is available, it is easy to evaluate the effect of arbitrary storage conditions on the internal local gas concentrations. A reaction–diffusion model, which incorporates both gas diffusion with sources and sinks due to respiration, seems the most appropriate model (Mannapperuma et al., 1991). The term *respiration–diffusion* model will be used to emphasize that respiration is the active conversion process under study.

Models describing gas diffusion and respiration have been reported in the literature for, e.g. apples (Mannapperuma et al., 1991; Rabus et al., 2001) and potato tubers (Abdul-Baki and Solomos, 1994). For these commodities the shape can easily be approximated by a sphere or a cylinder and, hence, the diffusion equations can be solved analytically for a constant respiration rate, or by means of a simple finite difference scheme for a Michaelis–Menten type of kinetics. Mannapperuma et al. (1991) proposed a steady-state spherical mathematical model based on simultaneous gas diffusion and chemical reaction to represent the gas exchange of 'Golden Delicious' apples stored in controlled atmospheres. Abdul-Baki and Solomos (1994) solved the diffusion equation under steady-state conditions, approximating the skin and the tissue of a potato tuber, respectively, by a hollow metabolically inert cylindrical shell and a metabolically active solid cylinder. Rabus et al. (2001) constructed a respiration–diffusion model to study the development of internal browning in relation to the internal O_2 and CO_2 concentration in 'Braeburn' apples stored under various ambient atmospheres and temperatures.

In the aforementioned models, reasonable assumptions concerning fruit shape and presence or absence of respiration and internal gas gradients were made to simplify the calculations of the internal gas concentrations. However, when the shape of the product is irregular (e.g. pears), the respiration of the biological sample is high and both the skin and the tissue cause considerable gas gradients, then the solution of the reaction–diffusion equation becomes more complex, and numerical techniques, such as finite elements, are needed to solve the problem. No attempt has been made so far in the literature to develop and solve such a complex model.

The objective of this paper is to construct and validate a respiration–diffusion model for 'Conference' pears, based on respiration parameters and gas diffusion coefficients for pear skin and tissue determined in previous research. This model should be seen as a first step towards the construction of a generic model, which unravels the true biochemical triggers causing internal tissue browning and the development of cavities. Moreover, the strategy to construct a respiration model is not restricted to pears, but is widely applicable to other horticultural produce.

2. Materials and methods

2.1. Fruit material

Pears (*P. communis* L. cv. Conference) were harvested in September 2000 at the pre-climacteric stage at the Nationale Proeftuin voor Grootfruit in Velm (Belgium), cooled and stored according to commercial protocols for a period of 21 days at 20% O_2, 0.03% CO_2 and $-1\,^{\circ}C$ preceding CA storage (2% O_2, 0.7% CO_2 at $-1\,^{\circ}C$) until they were used for the experiments.

2.2. Geometrical model reconstruction of the pear

In the respiration–diffusion models for apples proposed by Mannapperuma et al. (1991) and Rabus et al. (2001) the shape of the fruit was approximated by a sphere and, hence, using a spherical coordinate system the differential equations could be solved analytically. For pears, no simple shape approximation exists and it was necessary to fully reconstruct the three-dimensional shape of the fruit with a computer vision system for shape description (Jancsók, 1999).

A typical image acquisition system includes a 3 CCD camera (KY-F 55B, JVC, Japan), lighting equipment (100W Philips Softone, The Netherlands), and a sample holder on a rotation table with a computer controlled stepper motor (Matsushita, Japan Servo Co Ltd, Japan). For the image acquisition, a PCI-based capture card (Matrox Comet, Matrox Inc., Canada) with a RGB daughter card was used.

Image processing software, programmed in MATLAB (The Mathworks Inc., USA) (Jancsók, 1999), was used to generate a finite element mesh of the pear starting from the raw pear images. The pear was placed on the rotation table and images were taken along the fruit equator (Fig. 1A). These images were segmented in object and background (Fig. 1B), and the contours of the pear fruit were extracted from the object on the image. Subsequently, a cubic spline (smooth polygonal approximation) was fitted to the contour. For surface reconstruction, only contour information was taken into account and, hence, 18 images from only one side of the object (0–180°) were taken. The number of images determines the accuracy of the reconstructed 3D geometry. The system was calibrated by taking images of objects with known dimensions and by calculation of the pixel resolutions in the X and Y direction. The extracted shape (contour) information of the individual images was combined to reconstruct a 3D geometrical model of the pear (Fig. 1C) (Jancsók et al., 1997, 2001). The shape descriptors were transferred to the ANSYS (ANSYS Inc., USA) finite element program package, where a mesh was generated on the pear volume (Fig. 1D).

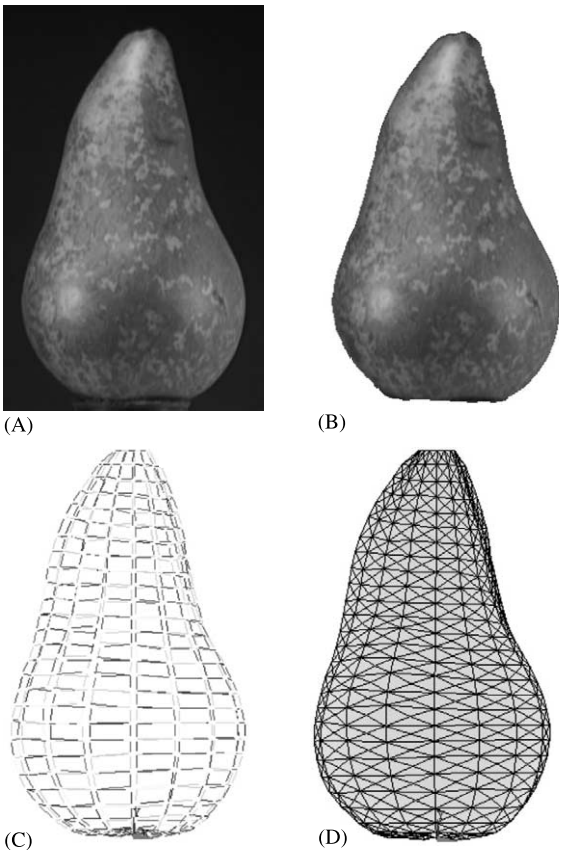

Fig. 1. Finite element grid generation of an intact pear based on an imaging system (Jancsók et al., 2001). Image of the pear taken with the CCD camera (A), segmentation of pear and background (B), three dimensional geometry of the pear with a patch surface (C), finite element mesh generated on the geometrical shape of the pear (D).

2.3. Model equations and parameters

In order to construct the model, three assumptions were made. First, ordinary diffusion caused by the concentration gradient was assumed to be the mode of gas transfer through skin and tissue. Second, the assumption of homogeneous and isotropic flesh was made. For reasons of simplicity no distinction was made between the different tissue structures in the pear. Finally, the skin thickness was considered negligible and all resistance to gas diffusion was included in the mass transfer coefficient. Both for O_2 and CO_2, a differential equation was established based on

Fick's second law of diffusion describing the changes in concentration of the respiratory gases in time (Eqs. (1) and (3)). Each equation consists of two terms. The first one contains the diffusion coefficient and describes the gas transport through the tissue. A second term describes the O_2 consumption or CO_2 production. The O_2 consumption is modelled with Michaelis–Menten kinetics including a non-competitive type of inhibition by CO_2 (Eq. (2)) (Lammertyn et al., 2001b):

$$\frac{\partial O_2}{\partial t} = D_{O_2}\nabla^2 O_2 - V_{O_2} \tag{1}$$

$$V_{O_2} = \frac{V_{m,O_2,cell} O_2}{(K_{m,O_2,cell} + O_2)\left(1 + \dfrac{CO_2}{K_{mn,CO_2,cell}}\right)} \tag{2}$$

with O_2 and CO_2, the CO_2 and O_2 concentration (mol m^{-3}), t the time (s); D_{O_2}, the gas diffusivity of O_2 in pear tissue (m^2 s^{-1}); V_{O_2}, the O_2 consumption rate (mol m^{-3} s^{-1}), ∇^2, the Laplace operator; $V_{m,O_2,cell}$, the maximum cellular aerobic O_2 consumption rate (mol m^{-3} s^{-1}); $K_{m,O_2,cell}$, the cellular Michaelis–Menten constant (mol m^{-3}) and $K_{mn,CO_2,cell}$, the cellular Michaelis–Menten constant for non-competitive inhibition of CO_2 on O_2 consumption (mol m^{-3}).

CO_2 production is composed of a fermentative part, which is inhibited at high O_2 concentrations, and an oxidative part, almost negligible at very low O_2 concentrations (Eq. (4)).

$$\frac{\partial CO_2}{\partial t} = D_{CO_2}\nabla^2 CO_2 + V_{CO_2} \tag{3}$$

$$V_{CO_2} = RQ_{cell} V_{O_2} + \frac{V_{m,f,CO_2,cell}}{1 + \dfrac{O_2}{K_{m,f,O_2,cell}}} \tag{4}$$

with D_{CO_2}, the CO_2 diffusivity in pear tissue (m^2 s^{-1}); V_{CO_2}, the CO_2 production (mol m^{-3} s^{-1}), RQ_{cell}, the cellular respiration quotient; $V_{m,f,CO_2,cell}$, the maximal cellular fermentative CO_2 production rate (mol m^{-3} s^{-1}); and $K_{m,f,O_2,cell}$, the inhibition constant of O_2 on the cellular fermentative CO_2 production (mol m^{-3}). The boundary conditions are given in Eqs. (5) and (6):

$$-D_{O_2}\frac{\partial O_2}{\partial n} = h_{O_2}(O_2 - O_{2,\infty}) \tag{5}$$

$$-D_{CO_2}\frac{\partial CO_2}{\partial n} = h_{CO_2}(CO_2 - CO_{2,\infty}) \tag{6}$$

with $CO_{2,\infty}$ and $O_{2,\infty}$ the ambient CO_2 and O_2 concentrations (mol m^{-3}); n the outward normal to the surface; h_{O_2} and h_{CO_2}, the convective mass transfer coefficients of O_2 and CO_2 between the pear and the ambient atmosphere (m s^{-1}), which incorporates the resistance of the pear skin.

We note that the proposed respiration model is not strictly based on biochemistry but is analogous to that used in Michaelis–Menten models for enzymes. More specifically, the mathematical expressions for the inhibition of fermentation by O_2 and the inhibition of O_2 consumption by CO_2 are not fully supported by biochemical mechanisms, but they do describe the data accurately.

In Table 1 an overview of the model parameters is given. For each parameter a letter indicates whether the parameter was measured on cell protoplasts (P), tissue disks (D) or on intact pears (I). Parameters inferred from literature are denoted by an L. A reference is provided which describes how the parameters were determined. The ideal gas law was used for the conversion of the units from gas molar concentrations to gas partial pressures and percentages.

2.4. Finite element solution

Since for pears, O_2 consumption depends on the CO_2 concentration and O_2 acts as an inhibitor of the fermentative CO_2 production (Lammertyn et al., 2001b), Eqs. (1) and (3) are coupled through Eqs. (2) and (4). Moreover, a non-linear relation exists between the partial deriviative of O_2 (and CO_2) with time and the O_2 (and CO_2) concentration. For realistic applications (complex geometries, non-linear boundary conditions, etc.) no analytical solution exists for the coupled non-linear equations and thus a numerical solution is needed. The finite element method is a flexible and accurate numerical technique to solve this type of partial differential equations. In the framework of the finite element method, the three dimensional

Table 1
Measured respiration–diffusion model parameters ±95% confidence limits and adapted respiration–diffusion model parameters

Parameter	Origin	Measured value ±95% confidence limits	Adapted model value
D_{O_2} ($m^2\ s^{-1}$)	D [1]	$1.71 \times 10^{-9} \pm 1.0 \times 10^{-9}$	5×10^{-9}
D_{CO_2} ($m^2\ s^{-1}$)	D [3]	$1.95 \times 10^{-8} \pm 1.5 \times 10^{-8}$	4×10^{-8}
h_{O_2} ($m\ s^{-1}$)	D [1]	$4.4 \times 10^{-7} \pm 2.2 \times 10^{-7}$	6×10^{-7}
h_{CO_2} ($m\ s^{-1}$)	D [3]	$1 \times 10^{-6} \pm 7.2 \times 10^{-7}$	7.5×10^{-7}
$V_{m,O_2,cell}$ ($mol\ m^{-3}\ s^{-1}$)	D [1]	$2.7 \times 10^{-4} \pm 1.8 \times 10^{-4}$	2×10^{-4}
$K_{m,O_2,cell}$ ($mol\ m^{-3}$)	P [2]	$3.0 \times 10^{-3} \pm 5.2 \times 10^{-4}$	0.05
$K_{mn,CO_2,cell}$ ($mol\ m^{-3}$)	I [2]	29.01 ± 8.86	14.51
$V_{m,f,CO_2,cell}$ ($mol\ m^{-3}\ s^{-1}$)	D [1]	$1.46 \times 10^{-4} \pm 7.88 \times 10^{-5}$	1.0×10^{-4}
$K_{m,f,O_2,cell}$ ($mol\ m^{-3}$)	I [2]	0.283 ± 0.070	2.83×10^{-4}
RQ_{cell}	I [2]	1	1

When confidence limits are omitted, the value was not measured but kept fixed. For each parameter a letter indicates whether the parameter was measured on cell protoplasts (P), tissue disks (D) or on intact pears (I). References are provided to indicate how the parameters were determined. $V_{m,f,CO_2,cell}$ was measured on pear disks stored under N_2 conditions according to Lammertyn et al. (2001a). [1] Lammertyn et al., 2001a; [2] Lammertyn et al., 2001b; [3] Lammertyn, 2001.

pear geometry is subdivided into elements with a tetrahedral shape, which are interconnected in a finite number, N, of nodal points. The number of elements and nodes depends on the pear geometry and the accuracy of the applied mesh. Typical numbers of elements and nodes used in this study are 7500 and 1626, respectively. In every element the unknown steady state gas concentrations are approximated by a first order interpolating polynomial. The Galerkin weighted residual method is applied as a spatial discretization technique, resulting in the following system of equations (Segerlind, 1984) for each respiratory gas.

$$Ku = f \tag{7}$$

with $u = [u_1\ u_2\ \ldots\ u_N]^T$ the overall nodal gas concentration vector, and K the $N \times N$ conductance matrix, and f an $N \times 1$ finite element load vector which is a function of both the nodal oxygen and carbon dioxide vector.

An existing MATLAB software package (Chamspack, Scheerlinck et al., 2000) was modified to solve the coupled non-linear reaction–diffusion equations. Finally, the model solutions were exported to the ANSYS (ANSYS Inc., Canonsburg, USA) finite element package for postprocessing.

A grid refinement study, carried out to assess the effect of grid refinement on the finite element solution, showed no difference in calculated gas concentrations when the number of elements was increased from 7500 to 13 623. To reduce the calculation time the mesh consisting of 7500 was used for further calculations, resulting in an approximate CPU time of 200 s per simulation.

2.5. Model validation

2.5.1. Gas exchange of a pear with its environment

In a first validation experiment, the simulation results of the respiration–diffusion model are compared with those of intact pear respiration measurements. A detailed decription of the experimental design, the measurement protocol and the results of the intact pear respiration measurements can be found in our earlier work (Lammertyn et al., 2001b). In that study the respiration measurements were carried out at 23, 15 and 7 °C and a Michaelis–Menten model including non-competitive CO_2 inhibition was fitted to these data. The temperature effect on respiration was modeled using an Arrhenius equation. Based on this Michaelis–Menten model, the respiratory behavior of intact pears at 20 °C, a temperature at which no raw data were measured, was calculated. These data, which will be called 'experimental data' from now on, represent the average pear O_2 consumption and CO_2 production at 20 °C and can be compared with the respiration rates simu-

lated at 20 °C with the reaction–diffusion model, as a validation of the latter.

As mentioned earlier, respiration measurements on intact pears reflect the total gas exchange of the fruit with its environment. This gas exchange occurs via the fruit skin. In steady-state conditions, the O_2 consumption and CO_2 production rates (mol kg^{-1} s^{-1}), a function of the ambient atmospheric conditions and temperature, are proportional to the total O_2 and CO_2 fluxes (mol s^{-1}) through the skin, respectively. The proportionality factor is the mass of the pear. Similarly, for the respiration–diffusion model, the gas exchange rate of the pear with its ambient atmosphere was calculated by integrating the gas flux over all finite elements at the boundary of the fruit using a Gauss–Legendre scheme (Segerlind, 1984).

$$f_G = \int_A h_G(G - G_\infty)dA \tag{8}$$

with A, the surface of the pear; h_G, the gas transfer coefficient at the boundary of the pear (m s^{-1}) reflecting the skin resistance to diffusion of gas G; f_G the flux of gas G (mol s^{-1}), and G, the gas concentration under the skin (mol m^{-3}) and G_∞, the ambient gas concentration (mol m^{-3}). In steady-state, the O_2 consumption and CO_2 production rates are equal to the respective fluxes divided by the mass of the pear. A pear density of 970 kg m^{-3} was determined with the method of Baumann and Henze (1983) and used to convert fluxes per kg to fluxes per volume and vice versa.

The gas exchange of one pear (mass 189 g) with its environment was simulated (Eq. (8)) at different environmental gas atmospheres. The simulations were carried out for a full factorial design of eight O_2 concentrations (0, 1, 2, 4, 8, 10, 15, 20%) and three CO_2 concentrations (0, 5, 15%) at 20 °C. For each combination of O_2 and CO_2 concentrations in the atmosphere, the O_2 production and CO_2 consumption rate were simulated. The simulations were performed starting with the initial parameter set (Table 1). Since $K_{mn,CO_2,cell}$ and $K_{m,f,O_2,cell}$ were not estimated in independent experiments, these two parameters were assigned an initial value equal to those of the intact pear respiration model.

A Michaelis–Menten model with non-competitive CO_2 inhibition (Eq. (2)) was also fitted to the simulated data. The parameters of the model were estimated with the non-linear regression algorithm of SAS/STAT, version 8.2 (SAS Institute Inc., USA).

2.5.2. Gas atmosphere under the skin

Another way to validate the prediction performance of the respiration–diffusion model is to measure the O_2 and CO_2 concentrations under the skin. This type of measurement focuses mainly on the validation of the convective mass transfer coefficients for both respiratory gases. Fifteen pears were stored under commercial storage conditions for a period of 9 months. A small volume (4.5 ml) plastic airtight respiration chamber was glued to the surface at the thickest part of the pear and sealed completely from the ambient atmosphere with vacuum grease (Mannapperuma et al., 1991). Subsequently, the pears were put in 1.8 l glass jars to equilibrate under their respective storage atmosphere. This atmosphere was kept constant by flushing the jars with the corresponding humidified gas mixture. Five pears were equilibrated at 100% N_2 and 20 °C. A second set of five pears was stored under shelf life conditions, 21% O_2, 0% CO_2 and 20 °C. The last set of five pears was equilibrated at the same gas conditions as the previous one, but at a temperature of 1 °C. After 60 h, a gas sample of 1 ml was withdrawn from each of the respiration chambers and analyzed with a micro-GC (Chrompack CP 2002, The Netherlands).

3. Results

3.1. Validation experiment 1: respiration of intact pears

The 'experimental data' on the O_2 consumption rate and the CO_2 production rate are plotted (lines) as a function of the O_2 and CO_2 concentrations in Fig. 2A and B. Since these 'experimental data' are interpolated model values at 20 °C (see Section 2.5.1) it was possible to plot them as lines instead of discrete points as is usually the case for experimental data. In Fig. 2A and B, the symbols

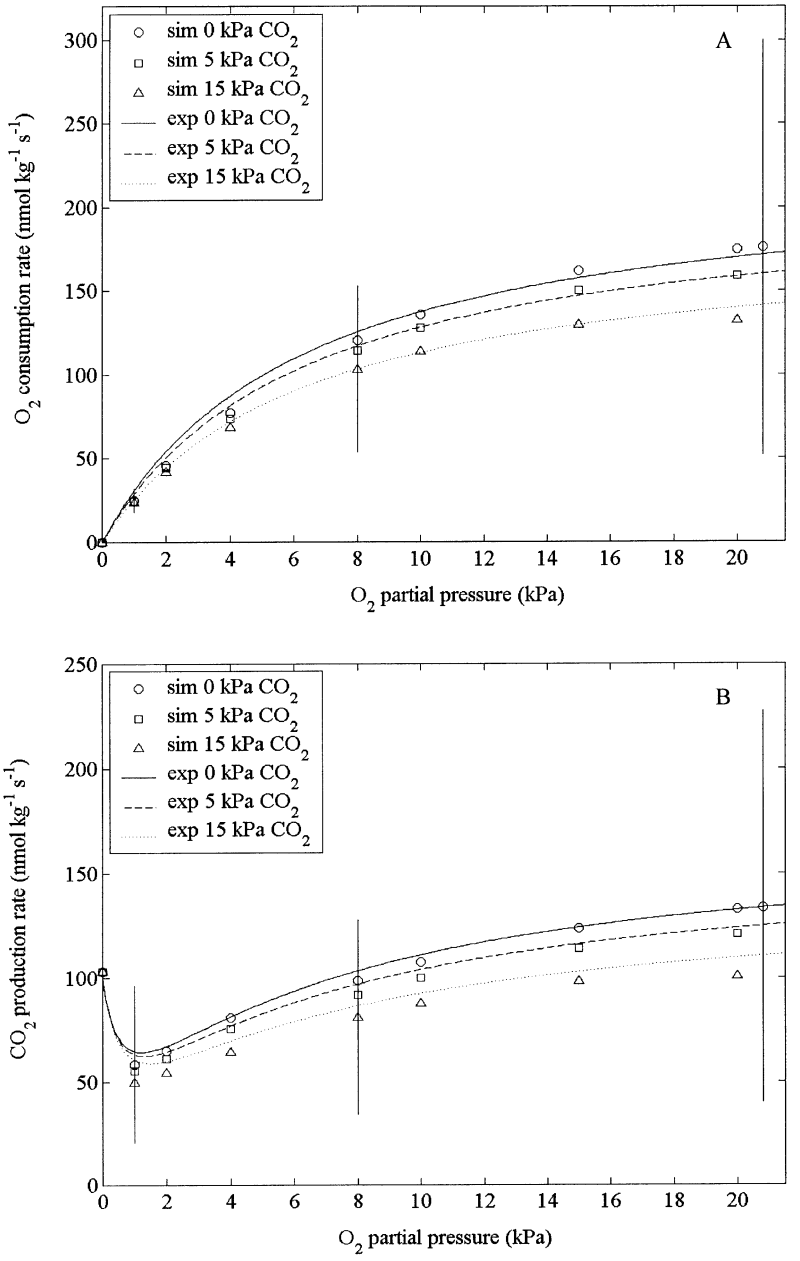

Fig. 2. Oxygen consumption rate (A) and CO_2 production rate (B) for intact pears as a function of the O_2 and CO_2 concentration (0, 5 and 15 kPa) at 20 °C. The lines represent the 'experimental data' obtained from a model interpolation of the data of Lammertyn et al., (2001b) as described in Section 2.5.1. The symbols represent the respiration rates simulated with the respiration–diffusion model. The vertical bars indicate the simulated value $\pm 2\sigma$.

represent the calculated values obtained with the respiration–diffusion model. The respiration–diffusion model values were only calculated for a limited number of O_2 and CO_2 combinations, since

it was too time consuming and computer intensive to calculate the respiration–diffusion model values over the whole O_2 concentration range for the three CO_2 concentrations at 20 °C.

$K_{mn,CO_2,cell}$ and $K_{m,f,O_2,cell}$ were not estimated from independent experiments and, therefore, an initial value needed to be assigned. The initial values were taken from the Michaelis–Menten respiration model for intact pears (Table 1). In advance, it was clear that these initial parameter values would be too large because they were estimated on intact pear gas exchange data which involve both respiration and diffusion processes. With the initial set of respiration–diffusion model parameters, simulations were carried out and compared with the 'experimental data'. In order to obtain a reliable set of parameters describing the combined effect of respiration and diffusion and to get information about the unknown Michaelis–Menten parameters at the cellular level, $K_{mn,CO_2,cell}$ and $K_{m,f,O_2,cell}$, the latter were adjusted manually to obtain the best correspondence between the 'experimental' and simulated data. In this respect, the simulations carried out here can be seen as an experiment to estimate unknown model parameters on the one hand, and as a validation of known parameters on the other. Since the Michaelis–Menten constants are hard to identify accurately in independent experiments (Versyck et al., 1997), it can be justified to adjust them first when parameter adjustments are carried out. Some of the other respiration–diffusion model parameters were adapted manually as well within their 95% confidence limits (Table 1) to improve the agreement between simulated and experimental data.

The resulting parameter set is given in Table 1. In Fig. 2A and B, the O_2 consumption and CO_2 production rates are shown as a function of the O_2 concentration for three CO_2 concentrations. The full lines correspond to the 'experimental data' and the symbols represent the simulated respiration rates.

All but one parameter adjustments fall within the corresponding 95% confidence limits. Only the O_2 diffusivity parameter (5×10^{-9} m^2 s^{-1}) exceeds the 95% confidence limits indicated in Table 1. The final $K_{m,O_2,cell}$ value used in the model is 16 times higher than the one measured on cell protoplasts in suspension. The $K_{mn,CO_2,cell}$ and $K_{m,f,O_2,cell}$ values, which were initially set to those determined from the intact pear respiration measurements, needed to be decreased considerably in order to obtain a good agreement between 'experimental' and simulated respiration rates. This might be expected, since these parameters were initially estimated from intact pear respiration measurements and, hence, contain information about the diffusion, as was illustrated in Lammertyn et al. (2001b). The initial set of parameters contained the $K_{m,O_2,cell}$ value measured on pear cell protoplasts in suspension. However, no model convergence was obtained when this value was used. The value was increased until convergence was obtained, ending up with a final $K_{m,O_2,cell}$ value being one order of magnitude higher than the one for cells. Again, this is not a surprising result as will be discussed later.

On the simulated O_2 consumption and CO_2 production rates (symbols in Fig. 2A and B), a Michaelis–Menten kinetics model including non-competitive inhibition by CO_2 was fitted and parameters were estimated. This model describes the total gas exchange (respiration and diffusion) of the fruit with their environment. The results are

Table 2
Michaelis–Menten parameters ±95% confidence limits fitted on the experimental data on intact pear respiration and fitted on the respiration rates simulated for intact pears with the respiration–diffusion model

Parameter	Parameter estimates of Michaelis–Menten model ±95% confidence limits	
	Experimental data	Simulated data
$V_{m,O_2,pear}$ (nmol kg^{-1} s^{-1})	220±24.5	242.2±10.00
$K_{m,O_2,pear}$ (kPa)	6.2±0.9	7.84±0.73
$K_{mn,CO_2,pear}$ (kPa)	70.7±21.6	63.5±10.2
$V_{m,f,CO_2,pear}$ (nmol kg^{-1} s^{-1})	99.74±20.5	102.7±3.5
$K_{m,f,O_2,pear}$ (kPa)	0.69±0.17	0.62±0.08
RQ_{pear} (–)	0.76±0.03	0.75±0.02

The index 'pear' indicates that those parameters were estimated from measurements on intact pears and not on cells as those presented in Table 1.

presented in Table 2. The parameters obtained in this way are compared with those estimated from intact pear respiration experiments described in Lammertyn et al. (2001b). The model parameters determined from the simulated data show a close agreement with the parameters estimated from the 'experimental data' on intact pear respiration. The values of the former are included in the 95% confidence limits of the latter.

It should be noted that for the simulations, always the same pear with the same diameter and weight was used and, hence, almost no biological variability is present compared with experimental data. This results in narrower confidence limits for the model parameters estimated from simulated data (Table 2).

3.2. Validation experiment 2: gas atmosphere under the skin

The previous experiments were not pure validation experiments, since two parameters were unknown and needed to be adapted. In this section, measurements of the gas atmosphere under the skin at different ambient atmospheres and temperatures are used to validate the respiration–diffusion model with the final set of parameters (Table 1). For each of three gas atmospheres, the O_2 and CO_2 concentrations under the skin were measured for five pears (Table 3) and simulated for one pear. The latter was sufficient since the gas concentration under the skin is mainly determined by the mass transfer coefficients (skin resistance) and, is therefore, independent of the pear shape. For all storage gas atmospheres, the average O_2 and CO_2 concentrations (five pears) under the skin fall within the 2σ limits (in analogy with 95% confidence limits) around the predicted value, indicating a good model performance. The $V_{m,O_2,cell}$ and $Vm,f,CO_2,cell$ parameters were calculated for 1 °C using Arrhenius' equation. Under the assumption that only those two model parameters are temperature dependent, the O_2 and CO_2 concentrations under the skin were simulated, to validate the model for other temperatures. The results in Table 3 suggest that a reasonable assumption was made and that the respiration–diffusion model is suited for predictions at other temperatures.

4. Discussion

In the present study, a respiration–diffusion model is constructed based on Fick's second law of diffusion. The respiration is described by means of Michaelis–Menten kinetics including non-competitive CO_2 inhibition. The gas transfer and respiration parameters were measured in Lammertyn et

Table 3
Experimental and simulated gas concentrations under the skin of pears, for different ambient gas atmospheres

	Ambient atmosphere					
	$O_2 = 20.8\%$, $CO_2 = 0\%$, $T = 20$ °C		$O_2 = 20.8\%$, $CO_2 = 0\%$, $T = 1$ °C		$O_2 = 0\%$, $CO_2 = 0\%$, $T = 20$ °C	
	O_2 (%)	CO_2 (%)	O_2 (%)	CO_2 (%)	O_2 (%)	CO_2 (%)
Pear 1	14.5	4.8	20.7	0.6	0.3	3.6
Pear 2	14.1	5.6	20.9	0.7	0.2	4.0
Pear 3	16.4	3.0	20.4	1.0	0.2	4.1
Pear 4	14.4	5.9	20.9	0.3	0.2	3.7
Pear 5	13.9	4.7	20.7	0.4	0.1	4.5
Mean	14.7	4.8	20.7	0.6	0.2	4.0
$\sigma_{experimental}$	1.0	1.1	0.20	0.27	0.071	0.36
Model	14.4	4.7	19.6	0.9	0	3.6
$\sigma_{simulation}$	2.4	2.6	0.59	0.58	0	2.2

The simulated values were calculated with the adapted parameter set of Table 1. σ denotes the standard deviation.

al. (2001a,b). Five model parameters need some extra discussion.

The first parameter that needs further attention is the respiration quotient, RQ. It is the ratio of the CO_2 production and the O_2 consumption rate. Theoretically, at the cellular level, the respiration quotient at the cellular level, RQ_{cell}, has a value close to 1 when no fermentation occurs in the cell. However, when the gas exchange of a pear is determined in a closed system, the respiration quotient, RQ_{pear}, typically has a value between 0.7 and 0.8 (De Wild and Peppelenbos, 2001), suggesting that more O_2 has been consumed than CO_2 has been produced. Lammertyn et al. (2001b) found a RQ_{pear} of 0.76 for respiration measurements on intact pears (Table 2). De Wild and Peppelenbos (2001) attributed the difference between RQ_{cell} and RQ_{pear} to the solubility of CO_2 in the water phase of the fruit tissue. In closed systems, RQ_{pear} is often underestimated due to underestimation of the CO_2 production. In this respiration–diffusion model the effect of CO_2 solubility is accounted for by the diffusion coefficient for CO_2 (Lammertyn, 2001). This coefficient describes the joint effect of CO_2 solubility in the water phase of fruit tissue and the CO_2 diffusion through the tissue.

The $K_{mn,CO_2,cell}$ and $K_{m,f,O_2,cell}$ were not measured on cell protoplasts in suspension or on tissue disks but the corresponding intact pear respiration values were used as initial values in the model. The initial respiration–diffusion parameters were adapted within their 95% confidence intervals to obtain a good agreement of the simulated respiration rates with the ones measured on intact pears. In the final set of parameters, $K_{mn,CO_2,cell}$ is two times and $K_{m,f,O_2,cell}$ is even one thousand times smaller than the initial value. Smaller values were expected since the initial parameter values were estimated from intact pear gas exchange data and not from the diffusion-free protoplast system.

To obtain model convergence, the final $K_{m,O_2,cell}$ value in the model had to be taken one order of magnitude higher than that measured on cell protoplasts in suspension. The manual adjustment of the $K_{m,O_2,cell}$ parameter can be justified for two reasons. First, as reported in literature it is difficult to identify accurately the Michaelis–Menten constant (Versyck et al., 1997), and hence a large uncertainty may exist. Second, cell protoplasts in suspension float around in their medium and have access to the surrounding O_2 dissolved in the medium. The gas exchange of the protoplasts with the medium is optimal; no diffusion barriers but the plasma membrane are present since cell protoplasts are deprived of their cell wall. As in pear tissue, clusters of lignified cells occur abundantly, the tissue structure can be considered as a network of macroscopic inter-cluster and microscopic intra-cluster aeration channels (Fig. 3). The gas diffusion in inter-cluster channels goes rapidly and all clusters have good access to these inter-cluster channels to exchange respiratory gases. However, gas diffusion within a cluster of cells is much slower. Not all cells of the cluster have equal access to the incoming O_2 and discharge the produced CO_2. Hence, O_2 and CO_2 gradients are established within a cluster of cells. This diffusion barrier caused by the cluster structure is absent in cell protoplasts in suspension. Therefore, the $K_{m,O_2,cells}$ value measured on cells is estimated too low and should be increased in the final respiration–diffusion model to that of one matching a system of clustered cells.

A final parameter that will be discussed is the O_2 diffusivity, although a similar discussion holds for D_{CO_2}. D_{O_2} was adapted here slightly beyond its 95% confidence limits. A possible interpretation might be as follows. Since no raw data were present at 20 °C, the Michaelis–Menten model describing the total gas exchange (intact pear respiration) of the fruit with their environment was interpolated to generate the average gas exchange behavior of pears at 20 °C. The respiration–diffusion parameters were adapted to fit closely these average experimental data on intact pear respiration. Here it was assumed that the model pear geometry represents the average pear shape, which might be a questionable assumption. Moreover, the whole simulation experiment of intact pear respiration was carried out on the same pear, which reduces the biological variability considerably. When D_{O_2} is kept within its 95% confidence limits, the simulated respiration rates deviate somewhat more from the average experimental data, but still within acceptable limits

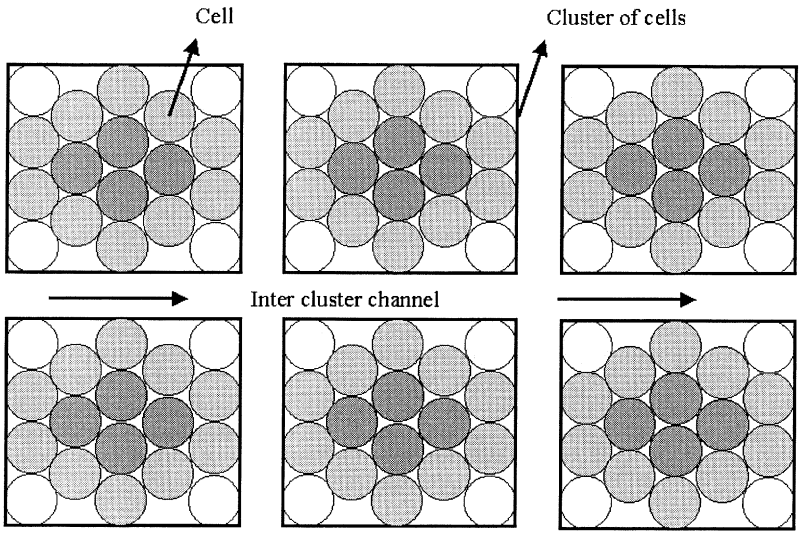

Fig. 3. Schematic representation of pear tissue structure. Cells are organized in clusters of lignified cells which are surrounded by inter cluster air channels and in which gas gradients occur. Darker cells experience more diffusion-limited gas transport.

considering the biological variability. The simulations would be more realistic if pears with different geometries are generated, for which the respiration rates are then simulated. Moreover, a different set of pears should be taken for each ambient atmosphere for which the respiration rates are simulated. This would closely resemble the biological variation (differences in shape, maturity, etc.) reflected in the results of the respiration experiments on intact pears.

When a Michaelis–Menten type of equation is used to describe a process such as gas exchange of fruit, which involves both gas diffusion and respiration, the estimated Michaelis–Menten parameters are much higher than those obtained when respiration is first uncoupled from the diffusion process and then described by means of Michaelis–Menten kinetics. This can be attributed to the dimensions of the system on which the parameter estimation is based. In the first case the process of gas diffusion has to be included in the model parameters, while in the second case, most of the diffusion effect is taken out and only respiration is described.

The respiration–diffusion model was used to simulate the O_2 consumption and CO_2 production rates of one pear as a function of eight O_2 and three CO_2 concentrations. These respiration rates describe the total gas exchange of the fruit with its environment. A Michaelis–Menten model, including non-competitive CO_2 inhibition, was fitted to the simulated data, and the obtained model parameters were used to reconstruct the three lower curves depicted in Fig. 4A and B for O_2 consumption and CO_2 production, respectively. In a similar way, the Michaelis–Menten parameters from the respiration–diffusion model were used to reconstruct the relation between respiratory gas rates and gas concentrations. These curves correspond to the three upper curves in Fig. 4A and B. When both groups of curves are compared for O_2 it is clear that the $K_{m,O_2,pear}$ value is much higher than the $K_{m,O_2,cell}$ value, because of the gas diffusion effect, whereas the difference between $V_{m,O_2,cell}$ and $V_{m,O_2,pear}$ is rather small. At very high O_2 levels the corresponding curves of both groups will have the same maximal respiration rate. The value of $K_{mn,O_2,cell}$ is only slightly smaller than that for $K_{mn,O_2,pear}$.

A comparison of the CO_2 production rate between both groups of curves reveals that again the maximal CO_2 production rates converge asymptotically to the same value. The $V_{m,f,CO_2,cell}$ is equal to $V_{m,f,CO_2,cell}$, and because of the model structure, they are independent of the CO_2 concentration. However, the $K_{m,f,O_2,cell}$ value in the

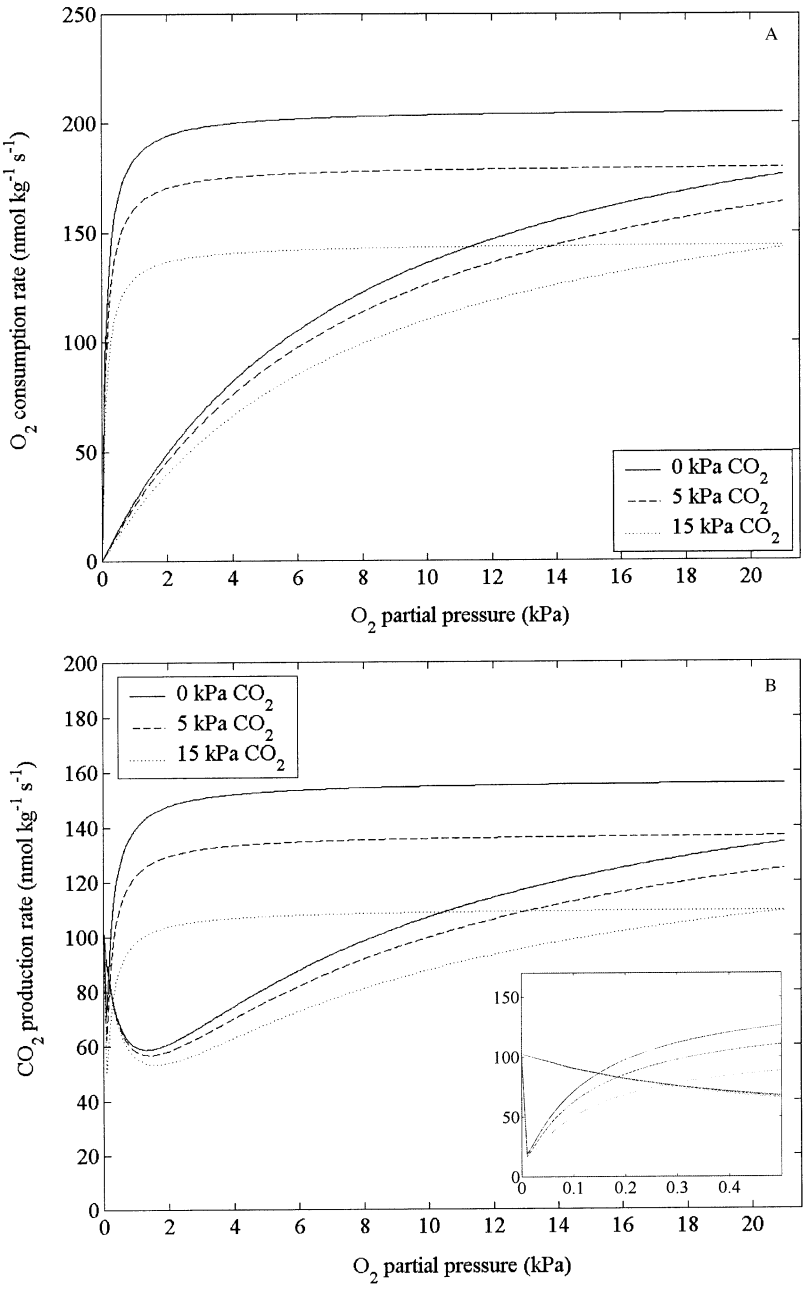

Fig. 4. (A) Michaelis–Menten kinetics for O_2 consumption simulated with the respiration–diffusion model for intact pears (upper three curves) and simulated with only the respiration parameters of the respiration–diffusion model (lower three curves). (B) Michaelis–Menten kinetics for CO_2 production simulated with the respiration–diffusion model for intact pears (upper three curves) and simulated with only the respiration parameters of the respiration–diffusion model (lower three curves). The inset in (B) is a magnification of the main figure and has the same units on the axis.

respiration–diffusion model is three orders of magnitude larger than the one for the Michaelis–Menten model to describe gas exchange of intact pears.

5. Conclusions

A respiration–diffusion model was constructed based on Fick's second law of diffusion. The respiration was described by a Michaelis–Menten kinetics, including non-competitive CO_2 inhibition of the O_2 consumption. The finite element technique was applied to numerically solve the system of coupled non-linear partial differential equations for a three dimensional pear geometry. The original idea was to combine in the reaction–diffusion model, 'diffusion-free' respiration parameters and 'respiration-free' diffusion parameters, which were determined in independent experiments. However, the 'diffusion-free' Michaelis–Menten constant for O_2 determined on protoplasts needed to be increased one order of magnitude to obtain convergence of the respiration–diffusion model. Hypothetically, this could be attributed to the presence of groups of lignified clustered cells abundantly present in pear tissue. In these clusters gas gradients, which are not accounted for by the respiration–diffusion model, may occur.

When a Michaelis–Menten type of equation was used to describe the respiration of whole fruit, the estimated Michaelis–Menten model parameters were higher than those obtained when respiration was first uncoupled from the diffusion process and then described by means of Michaelis–Menten kinetics.

The model was validated successfully in two independent experiments. In future research the presented respiration–diffusion model will be used to quickly calculate the internal gas concentration profiles and respiration rates of fruit stored under various storage atmospheres and to correlate the internal gas profiles with the incidence of core breakdown in 'Conference' pears. This respiration–diffusion model should be seen as a first step towards a generic model that describes the biochemistry and physical transport phenomena in pears and other horticultural products.

Acknowledgements

The Belgian Ministry of Small Enterprises, Traders and Agriculture and the Flemish Government are gratefully acknowledged for financial support (project S-5901). This research was also financially supported by European Union (EC-FAIR1-CT96-1803) and the Catholic University Leuven (IDO-project 00/008). Jeroen Lammertyn is Postdoctoral Fellow with the Flanders Fund for Scientific Research (FWO-Vlaanderen).

References

Abdul-Baki, A.A., Solomos, T., 1994. Diffusivity of carbon dioxide through the skin and flesh of 'Russet Burbank' potato tubers. J. Am. Soc. Hort. Sci. 119, 742–746.

Baumann, H., Henze, J., 1983. Intercellular space volume of fruit. Acta Hort. 138, 107–111.

Cameron, A.C., Talasila, P.C., Joles, D.W., 1995. Predicting film permeability needs for modified atmosphere packaging of lightly processed fruits and vegetables. HortScience 30, 25–34.

De Wild, H.P.J., Peppelenbos, H.W., 2001. Improving the measurement of gas exchange in closed systems. Postharvest Biol. Technol. 22, 111–119.

Jancsók, P., 1999. Geometrical model generation for finite element meshes of biological products based on digital image processing. Ph.D. thesis, Faculteit Landbouwkundige en Toegepaste Biologische Wetenschappen, Katholieke Universiteit Leuven.

Jancsók, P., Nicolaï, B.M., Coucke, P., De Baerdemaeker, J., 1997. 3D finite element model generation of fruits based on image processing. In: Munack, A., Tantau, H. (Eds.), Mathematical and Control Application in Agriculture and Horticulture, 28 September–2 October 1997, Hannover, Germany, pp. 131–135.

Jancsók, P., Clijmans, L., Nicolaï, B.M., De Baerdemaeker, J., 2001. Investigation of the effect of shape on the acoustic response of 'Conference' pears by finite element modelling. Postharvest Biol. Technol. 23, 1–12.

Lammertyn, J., 2001. A respiration–diffusion model to study core breakdown in Conference pears. Ph.D. thesis 494, Faculty of Agricultural and Applied Biological Sciences, Catholic University Leuven.

Lammertyn, J., Scheerlinck, N., Verlinden, B.E., Schotsmans, W., Nicolaï, B.M., 2001a. Simultaneous determination of oxygen diffusivity and respiration in pear skin and tissue. Postharvest Biol. Technol. 23, 93–104.

Lammertyn, J., Franck, C., Verlinden, B.E., Nicolaï, B.M., 2001b. Comparative study of the O_2, CO_2 and temperature effect on respiration between 'Conference' pear cell proto-

plasts in suspension and intact pears. J. Exp. Bot. 362, 1769–1777.

Mannapperuma, J.D., Singh, R.P., Montero, M.E., 1991. Simultaneous gas diffusion and chemical reaction in foods stored in modified atmospheres. J. Food Eng. 14, 167–183.

Peppelenbos, H.W., 1996. The use of gas exchange characteristics to optimise CA storage and MA packaging of fruits and vegetables. Ph.D. thesis, Landbouw Universiteit Wageningen.

Rabus, C., Streif, J., Bangerth, F., 2001. Simulation model for the calculation of internal gas exchange in apple fruits. Acta Hort. 553, 595–597.

Rajapakse, N.C., Banks, N.H., Hewett, E.W., Cleland, D.J., 1990. Development of oxygen concentration gradients in flesh tissues of bulky plant organs. J. Am. Soc. Hort. Sci. 115, 793–797.

Scheerlinck, N., Verboven, P., Stigter, J.D., De Baerdemaeker, J., Van Impe, J.F., Nicolaï, B.M., 2000. Stochastic finite element analysis of coupled heat and mass transfer problems with random field parameters. Numer. Heat Tr. B-Fund. 37, 309–330.

Segerlind, L., 1984. Applied Finite Element Analysis. Wiley, New York.

Versyck, K.J., Claes, J.E., Van Impe, J.F., 1997. Practical identification of unstructured growth kinetics by application of optimal experimental design. Biotechnol. Progress 13, 524–531.